University of Kent

Kent Academic Repository

Abooali, Maryam, Schlichtner, Stephanie, Lei, Xi, Aliu, Nijas, Ruggiero, Sabrina, Loges, Sonia, Ziegler, Martin, Hertel, Franziska, Volckmar, Anna-Lena, Stenzinger, Albrecht and others (2025) ***Intracellular and extracellular activities of V-domain Ig-containing suppressor of T cell activation (VISTA) modulated by immunosuppressive factors of tumour microenvironment.*** **Cancer Letters, 616 . ISSN 0304-3835.**

Downloaded from

https://kar.kent.ac.uk/108856/ The University of Kent's Academic Repository KAR

The version of record is available from

https://doi.org/10.1016/j.canlet.2025.217581

This document version

Publisher pdf

DOI for this version

Licence for this version

CC BY (Attribution)

Additional information

Versions of research works

Versions of Record

If this version is the version of record, it is the same as the published version available on the publisher's web site. Cite as the published version.

Author Accepted Manuscripts

If this document is identified as the Author Accepted Manuscript it is the version after peer review but before type setting, copy editing or publisher branding. Cite as Surname, Initial. (Year) 'Title of article'. To be published in ***Title of Journal*** , Volume and issue numbers [peer-reviewed accepted version]. Available at: DOI or URL (Accessed: date).

Enquiries

If you have questions about this document contact ResearchSupport@kent.ac.uk. Please include the URL of the record in KAR. If you believe that your, or a third party's rights have been compromised through this document please see our Take Down policy (available from https://www.kent.ac.uk/guides/kar-the-kent-academic-repository#policies).

Cancer Letters 616 (2025) 217581



Contents lists available at ScienceDirect

Cancer Letters

journal homepage: www.elsevier.com/locate/canlet



Original Articles



Intracellular and extracellular activities of V-domain Ig-containing suppressor of T cell activation (VISTA) modulated by immunosuppressive factors of tumour microenvironment

Maryam Abooali [a], Stephanie Schlichtner [b,c,d], Xi Lei [a], Nijas Aliu [e], Sabrina Ruggiero [f], Sonia Loges [b,c,d], Martin Ziegler [b,c,d], Franziska Hertel [b,c,d], Anna-Lena Volckmar [g], Albrecht Stenzinger [g,h], Petros Christopoulos [i,j,k], Michael Thomas [i,j,k], Elena Klenova [l], N. Helge Meyer [m], Stergios Boussios [n,o,p,q,r], Nigel Heaton [s], Yoh Zen [s], Ane Zamalloa [s], Shilpa Chokshi [t,u], Luca Urbani [u], Sophie Richard [u], Kavitha Kirubendran [u], Rohanah Hussain [v], Giuliano Siligardi [v], Dietmar Cholewa [f], Steffen M. Berger [f], Inna M. Yasinska [a], Elizaveta Fasler-Kan [f,*], Vadim V. Sumbayev [a,**]

[a] *Medway School of Pharmacy, Universities of Kent and Greenwich, Chatham Maritime, UK*
[b] *DKFZ-Hector Cancer Institute at the University Medical Center Mannheim, Mannheim, Germany*
[c] *Division of Personalized Medical Oncology (A420), German Cancer Research Center (DKFZ), Heidelberg, Germany*
[d] *Department of Personalized Oncology, University Hospital Mannheim, Medical Faculty Mannheim, University of Heidelberg, Mannheim, Germany*
[e] *Department of Human Genetics, Children's Hospital, Inselspital, University of Bern, Bern, Switzerland*
[f] *Department of Pediatric Surgery, Children's Hospital, Inselspital Bern, University of Bern and Department of Biomedical Research, University of Bern, Bern, Switzerland*
[g] *Institute of Pathology, Heidelberg University Hospital, Heidelberg, Germany*
[h] *Translational Lung Research Center (TLRC) Heidelberg, Member of the German Center for Lung Research (DZL), Heidelberg, Germany*
[i] *Department of Thoracic Oncology, Thoraxklinik, Heidelberg University Hospital, Heidelberg, Germany*
[j] *National Center for Tumor Diseases (NCT), NCT Heidelberg, a Partnership between DKFZ and Heidelberg University Hospital, Heidelberg, Germany*
[k] *Translational Lung Research Center Heidelberg (TLRC-H), Member of the German Center for Lung Research (DZL), Heidelberg, Germany*
[l] *School of Life Sciences, University of Essex, Colchester, UK*
[m] *Division of General and Visceral Surgery, Department of Human Medicine, University of Oldenburg, Oldenburg, Germany*
[n] *Faculty of Medicine, Health and Social Care, Canterbury Christ Church University, Canterbury, CT1 1QU, Kent, UK*
[o] *Faculty of Life Sciences & Medicine, School of Cancer & Pharmaceutical Sciences, King's College London, Strand, London, WC2R 2LS, UK*
[p] *Kent Medway Medical School, University of Kent, Canterbury, CT2 7LX, Kent, UK*
[q] *Department of Medical Oncology, Medway NHS Foundation Trust, Gillingham, ME7 5NY, Kent, UK*
[r] *AELIA Organization, 9th Km Thessaloniki-Thermi, 57001, Thessaloniki, Greece*
[s] *Institute of Liver Studies, King's College Hospital, Denmark Hill, London, UK*
[t] *Peninsula Medical School, Faculty of Health, University of Plymouth, UK*
[u] *Roger Williams Institute of Liver Studies, School of Immunology & Microbial Sciences, Faculty of Life Sciences and Medicine, King's College London, Foundation for Liver Research and King's College Hospital, London, UK*
[v] *Beamline 23, Diamond Light Source, Didcot, UK*

A B S T R A C T

V-domain Ig-containing suppressor of T cell activation (VISTA) is a unique immune checkpoint protein, which was reported to display both receptor and ligand activities. However, the mechanisms of regulation of VISTA activity and functions by factors of tumour microenvironment (TME) remain unclear and understanding these processes is required in order to develop successful personalised cancer immunotherapeutic strategies and approaches. Here we report for the very first time that VISTA interacts with another immune checkpoint protein galectin-9 inside the cell most likely facilitating its interaction with TGF-β-activated kinase 1 (TAK1). This process is required for protection of lysosomes, which is crucial for many cell types and tissues. We found that VISTA expression can be differentially controlled by crucial factors present in TME, such as transforming growth factor beta type 1 (TGF-β) and hypoxia as well as other factors activating hypoxic signalling. We confirmed that involvement of these important pathways modulated by TME differentially influences VISTA expression in different cell types. These networks

* Corresponding author.
** Corresponding author.
E-mail addresses: elizaveta.fasler@insel.ch (E. Fasler-Kan), V.Sumbayev@kent.ac.uk (V.V. Sumbayev).

https://doi.org/10.1016/j.canlet.2025.217581
Received 26 December 2024; Received in revised form 18 February 2025; Accepted 19 February 2025
Available online 20 February 2025
0304-3835/© 2025 The Author(s). Published by Elsevier B.V. This is an open access article under the CC BY license (http://creativecommons.org/licenses/by/4.0/).

include: TGF-β-Smad3 pathway, TAK1 (TGF-β-activated kinase 1) or apoptosis signal-regulating kinase 1 (ASK1)-induced activation of activating transcription factor 2 (ATF-2) and hypoxic signalling pathway. Based on this work we determined the five critical functions of VISTA and the role of TME factors in controlling (modulating or downregulating) VISTA expression.

1. Introduction

Immune checkpoint proteins and small molecular weight compounds produced by malignant and non-cancerous cells recruited to the tumour microenvironment (TME) determine the ability of malignant tumours to escape patient's immune surveillance [1]. These immune checkpoints engage in crosslinks forming an immune evasion machinery which creates immunosuppressive TME [2,3]. In order to establish successful approaches for personalised targeted immunotherapy of human cancers, a deep understanding of the cross-links between immune evasion network pathways is required. However, biochemical functions and mechanisms regulating expressions of various immune checkpoint proteins remain unclear and require extensive research. One of such proteins is known as V-domain Ig-containing suppressor of T cell activation (VISTA). This is a unique protein which can display both receptor and ligand activities [4,5]. When acting as a receptor on the surface of T cells, VISTA can be involved in alteration of plasma membrane potential of T cells thus leading to impairing the capability of cytotoxic T cells to inject proteolytic enzyme granzyme B into the target cells [6]. This leads to a release of granzyme B from acidic granules into cytoplasm of cytotoxic T cells, where granzyme B gets activated and thus induces apoptosis of cytotoxic T cells, which produced it [6]. These effects are caused by ligand-receptor interactions of VISTA with another immune checkpoint protein galectin-9 which acts as a ligand for VISTA [6].

VISTA (as a receptor) can also interact with VSIG-3 (ligand) mediating T cell suppressive responses [7,8]. When VISTA is located on the surface of cancer or myeloid-derived suppressor cells (MDSCs) it can also display ligand properties [9]. Most likely there are several receptors recognising VISTA as a ligand, but so far only one was discovered, P-selectin glycoprotein ligand 1 (PSGL-1), which can recognise VISTA only under acidic pH similar to the one of TME [10]. This interaction most likely plays a role in T cell suppression. Other receptors of VISTA remain to be identified.

It is, however, important to mention, that in some cells VISTA does not really get translocated onto the cell surface. This applies to for example acute myeloid leukaemia monocytes or non-malignant human bronchial epithelial cells [11,12]. Despite VISTA is highly expressed in these cells, most of the protein is localised inside the cell and even T cell attack may not provoke VISTA translocation onto the cell surface.

Expression of VISTA was found to be directly regulated on one hand by hypoxia-inducible factor 1 (HIF-1) transcription complex and on the other [13] – by transforming growth factor beta type 1 (TGF-β)-Smad3 pathway [11,14]. However, TGF-β downstream responses appear to be cell type specific and differential. In some cell types, TGF-β induces expression of VISTA while in other cell types it can heavily downregulate (but not attenuate) VISTA expression [11,14].

These regulation mechanisms are most likely associated with the roles of VISTA in developing immunosuppressive TME, however, the underlying biochemical mechanisms and biological reasons for such differential effects remain unclear.

Obviously, VISTA has intracellular functions given its cellular distribution in various cell types [15]. And based on observations outlined above, we hypothesised that differential localisation and regulation of VISTA expression are associated with its intracellular and extracellular functions.

Here we report for the very first time that VISTA interacts with galectin-9 inside the cells most likely facilitating its interaction with TGF-β-activated kinase 1 (TAK1). This process is required for protection of lysosomes, which is especially important in large number of cell types. TGF-β-induced expression of VISTA is controlled via Smad3 pathway. While downregulation is triggered by TGF-β-induced TAK1 activation. TAK1 pathway activates transcription factor ATF-2 which interacts with promoter region of *VSIR* (VISTA gene) causing repression of VISTA expression. Importantly, ATF-2 can also block expression of VISTA induced by both HIF-1 and Smad3.

Downregulatory effects of TAK-1/ATF-2 pathway are observed mainly in the cells where VISTA is located inside the cell, so that galectin-9 can be released and complexed with Tim-3 for secretion aiming to suppress cytotoxic immune attacks. If cells translocate VISTA onto the surface – much higher concentrations of TGF-β will be required to block expression of this protein. On the cell surface VISTA plays a major role as immune checkpoint protein suppressing anti-cancer immunity and T cell functions.

Importantly, different types of cancers display differential VISTA expression responses determined by the intracellular and extracellular roles of VISTA. For example, in pulmonary and breast adenocarcinomas VISTA is used as immune checkpoint protein and as such its expression is upregulated by physiological/pathophysiological concentrations of TGF-β. While in hepatocellular carcinoma, VISTA expression is downregulated by TGF-β, so that these cells can secrete high levels of galectin-9 upon T cell attack.

2. Materials and Methods

2.1. Materials

Cell culture media, foetal bovine serum, supplements and basic laboratory chemicals were purchased from Sigma (Suffolk, UK). Microtiter plates for ELISA were obtained from Nunc (Roskilde, Denmark). Rabbit antibodies against VISTA (ab243891, which showed excellent capability to recognise both human and mouse VISTA in our experiments), galectin-9 (ab69630), phospho-S423/S425-Smad3 (ab52903), ATF-2 (ab32160), TAK1 (ab109526), ASK1 (ab45178), HIF-1α (ab51608) and CD3 (ab21703) as well as mouse antibody against HIF-1α (ab1) were purchased from Abcam (Cambridge, UK). Mouse antibody against β-actin (66009-1-Ig) was purchased from Proteintech (Manchester, UK). Goat anti-mouse and anti-rabbit fluorescently-labelled dye secondary antibodies were obtained from Li-COR (Lincoln, Nebraska USA). Mouse anti-Smad3 antibody (H00004088-M07), ELISA-based assay kits for the detection of VISTA, galectin-9, PD-L1 and TGF-β were purchased from Bio-Techne (R&D Systems, Abingdon, UK). Anti-Tim-3 mouse monoclonal antibody was described before [16]. All other chemicals used in this study were of the highest grade of purity and commercially available.

2.2. Cell lines and primary human cells

Cell lines used in this work were purchased from either European Collection of Cell Cultures, American Tissue Culture Collection or CLS Cell Lines Service GmbH. Cell lines were accompanied by authentication test certificates. BEAS-2B normal bronchial epithelium cells, LN18 human glioblastoma cells, HuH7 hepatocellular carcinoma cells and Calu6 pulmonary carcinoma cells were cultured using DMEM medium supplemented with 10 % foetal bovine serum, penicillin (50 IU/ml), and streptomycin sulfate (50 μg/ml). Jurkat T, THP-1 human acute myeloid leukaemia cells, K562 human chronic myeloid leukaemia cells, MCF-7 human breast cancer cells, PANC-1 human pancreatic ductal adenocarcinoma cells and HaCaT keratinocytes were cultured in RPMI 1640 medium supplemented with 10 % foetal bovine serum, penicillin (50 IU/ml), and streptomycin sulfate (50 μg/ml).

TALL-104 CD8-positive cytotoxic T lymphocytes, obtained from human acute lymphoblastic leukaemia (TALL), were cultured in ATCC-formulated Iscove's Modified Dulbecco's Medium. To make the complete growth medium we added 100 units/ml recombinant human IL-2; 2.5 μg/ml human albumin; 0.5 μg/ml D-mannitol and foetal bovine serum to a final concentration of 20 % as well as penicillin (50 IU/ml), and streptomycin sulfate (50 μg/ml).

2.3. Cell lines were used for experiments between passages 5 and 15

Placental tissue (CVS, chorionic villus sampling) and amniotic fluid samples were collected after obtaining informed written consent from 5 patients (pregnant women) in each case at the University Hospital Bern. Cells were prepared and cultured as described before [17,18]. Briefly, CVS were then washed with PBS, treated with 270 U/ml of collagenase type 2 (Sigma, Buchs, Switzerland) for 50 min at 37 °C and washed twice with PBS. After this, cells were re-suspended and cultured in CHANG medium (Irvine Scientific, Irvine, USA) according to the manufacturer's protocol. Amniotic fluid samples were centrifuged, followed by resuspension of the cell pellets in CHANG medium. The first medium change was performed after 5 days of incubation at 37 °C. The medium was then changed every second day until the number of cells was considered sufficient. Cells were cultured for 2–3 weeks in up to 3 passages, within which they were used for experiments.

2.4. Mice

Organs of two male and two female 11-week old C57BL/6 mice were isolated and tissue lysis was performed in order to conduct Western blot analysis. Animals were housed and experiments carried out in accordance with the institutional guidelines of German for the welfare of animals in experimental neoplasia and were approved by the local licensing authority (Behörde für Soziales, Gesundheit, Familie, Verbraucherschutz; Amt für Gesundheit und Verbraucherschutz). Housing, breeding, and experiments were performed under a 12 h light–dark cycle and standard laboratory conditions (22 ± 1 °C, 55 % humidity, food, and water, and 150–400 lx light intensity during the light phase). Animals were handled by authorised personnel in accordance with the Declaration of Helsinki protocols.

2.5. Human pulmonary carcinoma organoids

Samples taken from a patient with predominantly papillary pulmonary adenocarcinoma following informed written consent were obtained from the Thoraxklinik Heidelberg and processed for organoid cultivation. Samples contained both malignant tumour as well as corresponding healthy tissue. Tumour and healthy tissue of a single sample were processed. Tissues were cut into very small pieces and cells were collected. Tumour tissue was kept for processing in 4.8 ml complete advDMEM (HEPES & GlutaMAX 1 %), healthy tissues - in 1.8 ml complete advDMEM. Both types of samples were then processed using digestion enzymes: 25 μl DNAse, 250 μl collagenase/dispase (for tumour); 200 μl collagenase/dispase (for healthy tissues) and 5 μl rock-inhibitor, in an incubator with constant rotation for either 45 min (tumour) or 60 min (healthy tissue).

Samples were then filtered, washed with PBS and incubated with 1 ml ammonium-chloride-potassium (ACK) lysis buffer for 1 min. After incubation samples were washed again and re-suspended in a medium containing matrigel/BME + organoid medium including rock-inhibitor. Cells were then plated at a volume of 100 μl of re-suspended tissue. The plates were incubated at 37 °C for 30 min in order to solidify matrigel and 1.5 ml of organoid medium containing rock-inhibitor were added. Samples were kept in a standard incubator and medium was changed twice a week. Prior to cell lysis for Western blot analysis the matrigel needed for organoid cultivation was removed and standard cell lysis was performed. Preparation of organoids and their use in experiments were approved by the ethics commission II of the University Heidelberg (Medical faculty Mannheim, 2023–651, December 19, 2023).

2.6. Human tissue samples

Primary human tumour tissue samples paired together with peripheral tissues (also called "normal" or "healthy" of the same patients) were collected surgically from 5 breast cancer patients treated at the Colchester General Hospital, following informed, and written consent taken before surgery. Paired normal (healthy) peripheral tissues were removed during macroscopic examination of a tumour by pathologists. Blood samples were collected before breast surgery from patients with primary breast cancer (PBC). Samples were also collected from healthy donors (individuals with no diagnosed pathology), which were used as control samples. Blood separation was done using buoyancy density method employing Histopaque 1119–1 (Sigma, St. Louis, MO) according to the manufacturer's instructions. Ethical approval documentation for these studies was obtained from the NRES Essex Research Ethics Committee and the Research & Innovation Department of the Colchester Hospitals University, NHS Foundation Trust [MH 363 (AM03) and 09/H0301/37]. Primary human tumour tissue samples paired together with peripheral tissues (also called "normal" or "healthy" of the same patients) were also collected surgically from 2 colorectal cancer liver metastasis (CRCLM) patients treated at Kings College Hospital, following informed, and written consent taken before surgery. This study was conducted in accordance with the Declaration of Helsinki and approved by the local Research Ethics Committee established by the Health Research Authority (REC reference 17/NE/0340; IRAS project ID 222302). Also, paired normal (non-malignant) peripheral tissues were isolated during macroscopic examination of tumours by pathologists. Blood samples were collected before surgery from corresponding patients.

2.7. Western blot analysis

Levels of VISTA, Tim-3, phospho-S423/S425 Smad-3, ATF-2, CD3, and TAK1 were measured by Western blot and compared to the amounts of β-actin (protein loading control), as described previously [3,14]. Li-Cor goat secondary antibodies conjugated with infrared fluorescent dyes, were used as described in the manufacturer's protocol for visualisation of specific target proteins (Li-Cor Odyssey imaging system was employed). Western blot data were quantitatively analysed using Image Studio software and values were subsequently normalised against those of β-actin.

2.8. Chromatin immunoprecipitation (ChIP)

ChIP was performed as described recently [11]. Briefly, 5 x 10^6 cells were used for immunoprecipitation. Cross-linking was then performed using 1.42 % formaldehyde and this was followed by quenching for 5 min with 125 mM glycine. After this, cells were washed twice with PBS and subjected to ChIP according to ChIP-IT high sensitivity kit (Active Motif) protocol. Immunoprecipitation was performed using anti-Smad3, anti-HIF-1α antibodies or ATF-2 monoclonal antibodies. Isotype control antibodies were used for a negative control IP. The epitopes recognised by these antibodies do not overlap with DNA and co-activator binding sites of these proteins. Immunoprecipitated DNA was then purified and subjected to quantitative real-time PCR (qRT-PCR) which was performed as outlined below. The following primers were designed using NCBI Primer-Blast primer designing tool: VISTA forward – 5′-GCCTACCACATACCAAGCCC-3′ and reverse: 5′- ATCGGCAGTTTAAA GCCCGT-3'; galectin-9 forward: 5′-TCTTGCAAAATATTCCCCTCTA-CAT-3'; reverse – 5′-AAATAATGGGGCTGGGCATTG-3'. These primers allow amplification of the fragments of promoter regions of corresponding genes, which surround Smad3-binding sites.

2.9. qRT-PCR analysis

To detect VISTA and galectin-9 mRNA levels we used qRT-PCR [11]. Total RNA was isolated using a GenElute™ mammalian total RNA preparation kit (Sigma-Aldrich) according to the manufacturer's instructions, followed by reverse transcriptase–polymerase chain reaction (RT-PCR) of a target protein mRNA (also performed according to the manufacturer's protocol). The following primers were used: VISTA: forward – 5′-GATGCACCATCCAACTGTGT-3′, reverse – 5′-GCAGAGGATTCCTACGATGC-3′; galectin-9, 5′-CTTTCATCACCACCATTCTG-3′, 5′-ATGTGGAACCTCTGAGCACTG-3′; actin: forward – 5′-TGACGGGGTCACCCACACTGTGCCCATCTA-3′, reverse – 5′-CTAGAAGCATTTGCGGTCGACGATGGAGGG-3′. This was followed by qRT-PCR. Reactions were performed using a LightCycler® 480 qRT-PCR machine and SYBR Green I Master kit (Roche, Burgess Hill, UK). The assay was performed according to the manufacturer's protocol. Values representing VISTA mRNA levels were normalised against those of β-actin.

2.10. On-cell western analysis

Cell surface levels of VISTA, galectin-9, TGF-β and PD-L1 proteins were analysed using on-cell Western analysis performed using a Li-COR Odyssey imager and the assay was performed in line with manufacturer's recommendations as previously described [11,14].

2.11. Enzyme-linked immunosorbent assays (ELISAs)

Levels of secreted (soluble) VISTA, galectin-9 and TGF-β were measured in cell culture media and PD-L1 quantities were also analysed in cell lysates, by ELISA using R&D Systems kits (see Materials section) according to manufacturer's protocols.

2.12. Analysis of HIF-1 DNA-binding activity

HIF-1 DNA-binding activity was measured by the method, which was described recently [3,17]. In brief, 96-well Maxisorp™ microtitre plates were coated with streptavidin and blocked with BSA. A volume of 2 pmol/well biotinylated 2HRE (HRE – hypoxia response element) containing oligonucleotide was immobilised by 1 h incubation at room temperature. The plates were then washed with TBST buffer (10 mM Tris-HCl, pH 8.0, 150 mM NaCl, 0.05 % Tween-20), followed by 1 h incubation with cell lysate at room temperature. The plate was again washed with TBST buffer and mouse anti-HIF-1α antibody (1:1000 in TBS with 2 % BSA) was added. After 1 h of incubation at room temperature the plate was washed with TBST buffer and then incubated with Li-Cor goat anti-mouse secondary antibody labelled with infrared fluorescent dye. After extensive washing with TBST, the plate was scanned using a Li-Cor Odyssey fluoroimager.

2.13. In vitro assay of VISTA-galectin-9-TAK1 as well as Tim-3-gelectin-9/VISTA-galectin-9 interactions

This assay was performed as described before for Tim-3-galectin-9 interactions with modifications [14,19]. TAK1 from resting and TGF-β-treated cells was first precipitated on Maxisorp ELISA plates. For this purpose ELISA plates were coated overnight with rabbit antibody against TAK1. Plates were then blocked with 2 % BSA. Extracts of the cells were then applied for 2 h at room temperature, followed by extensive washing with TBST buffer. Proteins were then extracted using 0.2 M glycine-HCl buffer (pH 2.0). Extracts were neutralised using lysis buffer and subjected to Western blot analysis (samples where not boiled in this case) using anti-galectin-9 and mouse anti-VISTA antibodies as described before and above. Alternatively, the format was subjected to measurement of bound galectin-9 and VISTA using an ELISA kit according to the manufacturer's protocol.

To analyse Tim-3-galectin-9 or VISTA-galectin-9 interactions, we immunoprecipitated galectin-9 on the plates as described before [14,19] and above. Then we applied extracts of resting and TGF-β-treated cells as described above/before [14,19]. Presence of Tim-3 or VISTA was verified using primary antibodies and interactions were visualised using Li-Cor secondary antibodies and plates were scanned using Li-Cor Odyssey fluoroimager.

2.14. Transfection of Smad3 siRNA and dominant-negative isoform of ASK1 (ΔN-ASK1) into BEAS-2B cells

Smad3 siRNA was a commercially available reagent purchased from Ambion (ID 107876) through Thermo Fisher Scientific. Random (mutated) siRNA, which was used as a negative control in all the knockdown experiments had the following sequence: UAC ACC GUU AGC AGA CAC C dTdT. siRNAs were transfected into BEAS-2B cells using DOTAP transfection reagent according to the manufacturer's protocol [17]. Successful Smad3 knockdown was verified by Western blot analysis. Plasmid encoding hemagglutinin (HA)-tagged ASK1 with kinase-dead domain (dominant-negative form – ΔN-ASK1) was a kind gift of Professor Ichijo (University of Tokyo, Tokyo, Japan). Plasmid was amplified in Escherichia coli XL10 Gold® (Stratagene Europe, Amsterdam, The Netherlands) and purified using GenElute™ plasmid purification kit according to the manufacturers protocol. Purified plasmids were transfected into BEAS-2B cells using DOTAP transfection reagent according to the manufacturer's protocol.

2.15. Granzyme B activity assays

Granzyme B activity in cell lysates was measured using a fluorometric assay based on the ability of the enzyme to cleave the fluorogenic substrate Ac-IEPD-AFC (Sigma-Aldrich) as described before [6].

2.16. Analysis of thiobarbiturate reactive species (TBRS) concentrations

TBRS were quantified using a previously described colorimetric assay [20].

2.17. Measurement of TAK1 and ASK1 kinase activities

Kinase activities of TAK1 and ASK1 were assayed by the method based on immunoprecipitation of these enzymes followed by analysis of phosphorylation of exogenous substrate—myeline basic protein (MBP) and estimated in nmol of the phosphate transferred per 1 min onto the MBP per 1 mg protein as described previously [21,22].

2.18. Analysis of enzymatic generation of N-formylkynurenine

IDO1/TDO activities (or enzymatic conversion of L-Trp into N-formylkynurenine, which was then further converted into LKU), were measured using a previously described method with minor modifications, which were also described recently [3,23]. In brief, cell or tissue lysates were added to the reaction mixture containing 50 mM potassium phosphate buffer (pH 6.5), 20 mM ascorbate, 100 μg/mL catalase and 2 mM L-Trp. The reaction was carried out at 37 °C for 60 min and terminated by adding 10 μL of 30 % (v/v) trichloroacetic acid to 160 μL of sample. Further operations were performed as previously described.

2.19. Detection of LKU

LKU was measured based on its ability to react with 4-dimethylaminobenzaldehyde [3]. Briefly, 160 μL of cell culture medium or blood plasma was supplied with 10 μL 30 % (v/v) trichloroacetic acid to each sample. Samples were then incubated for 30 min at 50 °C in order to hydrolyze N-formylkynurenine to LKU. Samples were then centrifuged at 3000 g for 10 min 100 μl of supernatants were transferred to wells of a 96-well flat-bottom plate and mixed with 100 μL of freshly prepared

Ehrlich's reagent (1.2 % w/v 4-dimethylaminobenzaldehyde in glacial acetic acid) followed for 10 min incubation at room temperature. Absorbance was measured using a microplate reader at 492 nm.

2.20. Fluorescent microscopy and flow cytometry

Cells were cultured overnight on 12 mm cover slips in 24-well plates and then fixed/permeabilised for 20 min with ice-cold MeOH/acetone (1:1). Cover slips were blocked for 1h at RT with 10 % goat serum in PBS. Cells were stained with anti-galectin-9, anti-Tim-3 or anti-VISTA antibodies overnight at 4 °C. The nuclei were stained with 4′,6-diamidino-2-phenylindole (DAPI). Analysis was conducted using Olympus microscope as described previously [12]. Images were collected and analysed using proprietary image acquisition software.

Flow cytometry experiments were performed as previously described [12,14]. Briefly, cells were collected and fixed with 2 % paraformaldehyde where applicable permeabilised with 0.1 % TX-100 (to measure total cellular protein levels). Cells were stained with anti-galectin-9, anti-Tim-3 or anti-VISTA antibodies. Mean fluorescence intensity of stained cells was measured and analysed using a FACSCalibur analyser and the CEllQuest Pro Software (Becton Dickinson, USA).

2.21. Statistical analysis

Each experiment was performed at least three times (unless otherwise indicated) in duplicate and statistical analysis, was conducted using a two-tailed Student's *t*-test. Statistical probabilities (p) were expressed as * when $p < 0.05$; **, $p < 0.01$ and *** when $p < 0.001$.

3. Results

3.1. Intracellular interactions of VISTA with galectin-9 most likely facilitates further interaction of galectin-9 with TAK1

In the first instance we asked how do cells, which naturally express high levels of VISTA but do not translocate it onto the cell surface respond to treatments with TGF-β in terms of VISTA levels and galectin-9 localisation. We used wild type BEAS-2B human bronchial epithelial cells, which express high levels of VISTA, as well as BEAS-2B cells, which underwent malignant transformation *in vitro* with the help of bracken fern alkaloid ptaquiloside as described recently [12]. Both cell types expressed high levels of VISTA and in both cases the expression was heavily downregulated by 2 ng/ml TGF-β (time of exposure to TGF-β was 16 h). Phospho-Smad-3 levels were significantly upregulated in both cell types suggesting that cells positively responded to treatment with TGF-β.

Importantly, expressions of other Smad-3-dependent immune checkpoints of interest were upregulated by TGF-β (this effect was applicable to galectin-9, PD-L1 and IDO-1 (Fig. 1A). We then assessed VISTA, galectin-9 and Tim-3 (receptor and possible trafficker/carrier of galectin-9 during translocation onto the cell surface and secretion) levels and co-localisation using IF microscopy in resting BEAS-2B cells and those treated for 16 h with TGF-β. We found that VISTA in resting cells was located close to galectin-9 while in TGF-β-treated cells galectin-9 was close to Tim-3 (Fig. 1B). Importantly, on the Western blot

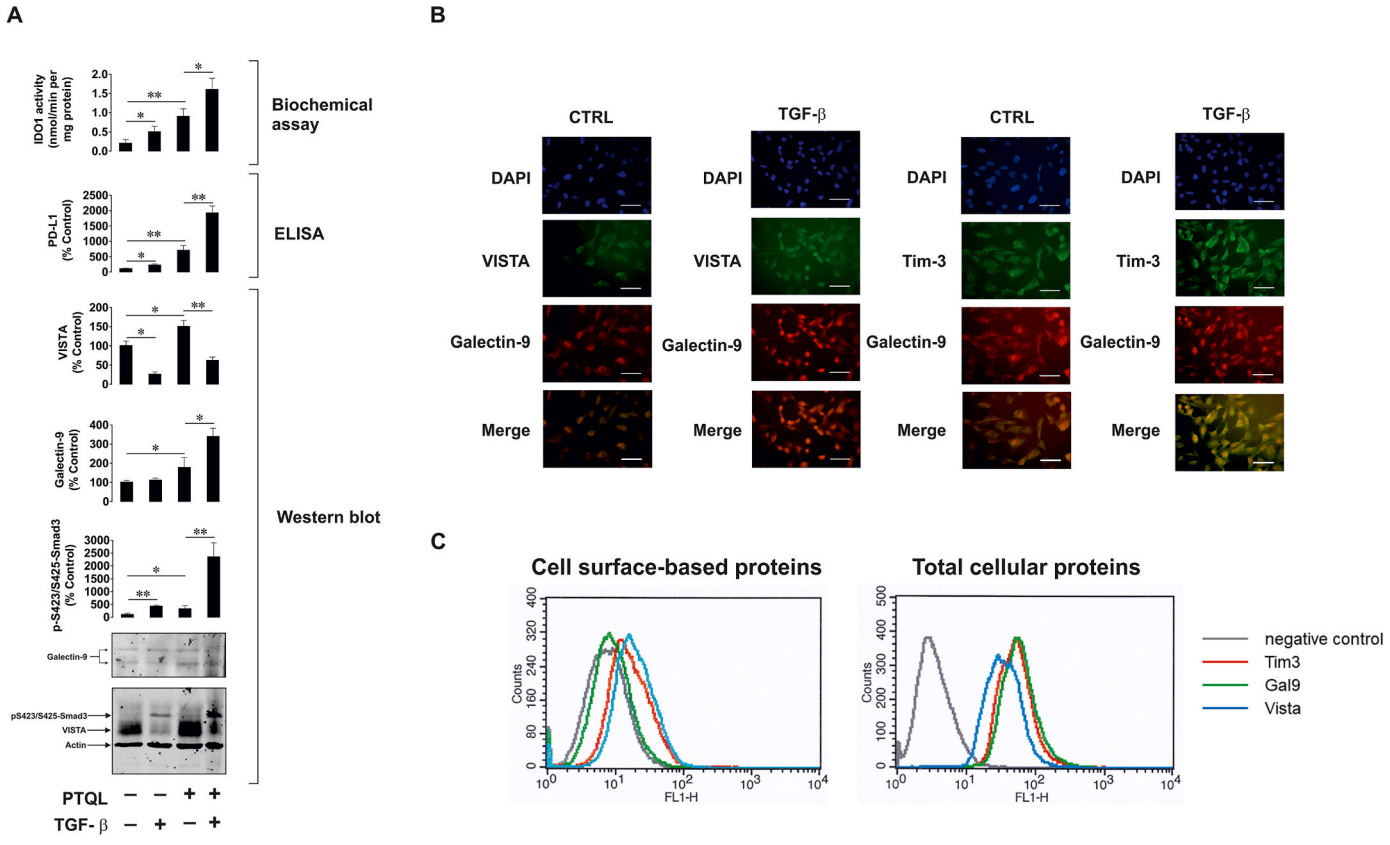


Fig. 1. TGF-β downregulates VISTA expression in BEAS-2B cells and impacts on co-localisation protein partner of galectin-9. (A) Normal and ptaquiloside-transformed BEAS-2B cells were exposed to 2 ng/ml TGF-β for 16 h. Cellular levels of VISTA, galectin-9 and phospho-S423/S425-Smad3 were measured by Western blot analysis. Cellular levels of PD-L1 were analysed by ELISA. IDO1 activity was measured using colorimetric assay. **(B)** Resting and TGF-β treated BEAS-2B cells were subjected to permeabilization followed be measurement of VISTA, galectin-9 and Tim-3 using immunofluorescent microscopy. **(C)** Cell surface and total cellular levels of VISTA, galectin-9 and Tim-3 were measured in BEAS-2B cells using FACS analysis as outlined in Materials and Methods. Images are from 1 experiment representative of 4, which gave similar results. Quantitative data are mean values ± SEM of 4 independent experiments. *$p < 0.05$ and **$p < 0.01$ between indicated events.

(Fig. 1A) we saw very high levels of VISTA, which were reduced upon exposure to TGF-β. In the case of IF microscopy, VISTA levels seemed low and were higher upon exposure of cells to TGF-β. This suggests that VISTA was engaged in protein-protein interactions and after exposure to TGF-β was released. As such its level was seen as upregulated on the IF microscopy, while its absolute levels were significantly downregulated according to the Western blot analysis. To further verify this, we measured cell surface-based VISTA, Tim-3 and galectin-9 in resting BEAS-2B cells *vs* total cellular amounts of these proteins using flow cytometry (Fig. 1C). We found that all the proteins were localised mainly inside the cells while total cellular levels of VISTA also seemed low, further confirming engagement of VISTA in intracellular protein-protein interactions reducing its capability to react with antibodies.

We then studied if this downregulation of VISTA expression is in line with galectin-9 release and secretion.

We co-cultured (direct co-culture) BEAS-2B cells with TALL-104 cytotoxic T cells in the ratio 1:1 for 16 h, as described before [14], in the absence or presence of 5 μg/ml TGF-β-neutralising antibody (Fig. 2A). We found that co-culture with T cells led to a high increase in TGF-β production (detected by ELISA) and downregulation of VISTA expression as measured by Western blot (Fig. 2B). Both effects were reduced by TGF-β neutralisation (Fig. 2B). It is important to mention that in neither of these 3 conditions secretion of VISTA was detectable by ELISA, suggesting presence of only cell-associated VISTA in all studied cultures. Importantly, presence of T cells triggered translocation of PD-L1 but not VISTA onto the cell surface (Fig. 2C). In line with this, granzyme B activity was clearly detectable (T cells injected it into BEAS-2B) in BEAS-2B cells co-cultured with T cells. This was in line with galectin-9 secretion levels. Neutralisation of TGF-β decreased galectin-9 secretion and led to a much higher granzyme B activity in BEAS-2B cells, when co-cultured with TALL-104.

To see if treatment with TGF-β can facilitate stimulated secretion of galectin-9, we exposed BEAS-2B cells for 16 h to 100 nM PMA, 2 ng/ml TGF-β or combination of both. We found that PMA induced barely detectable galectin-9 secretion, while TGF-β failed to trigger anything at all. But, the combination of both induced quite significant release of galectin-9 supporting hypothesis that TGF-β dependent reduction in VISTA expression helps to release galectin-9 (Fig. 2E).

In order to see if VISTA facilitates intracellular interactions of galectin-9 with TAK-1, we immunoprecipitated TAK1 as described in Materials and Methods in resting BEAS-2B and those exposed for 16 h to 2 ng/ml TGF-β (Fig. 3A). We found that TAK-1 was co-precipitated together with galectin-9 and VISTA in resting BEAS-2B cells, while these two proteins almost disappeared when TAK1 was immunoprecipitated from cells exposed to TGF-β as measured by Western blot analysis (Fig. 3B). The findings were confirmed when galectin-9 and VISTA were co-immunoprecipitated with TAK1 as measured by ELISA (Fig. 3C and D). We then sought to confirm if upon exposure of BEAS-2B cells to TGF-β, galectin-9 switches binding partner from VISTA to Tim-3. We immunoprecipitated galectin-9 on the ELISA plates and measured if VISTA and/or Tim-3 were co-precipitated with it (Fig. 3E). We found that in resting cells VISTA was mainly co-precipitated with galectin-9, while in TGF-β-treated cells, galectin-9 was mainly interacting with Tim-3 (Fig. 3F), which is in line other observations shown above suggesting the biological reason for downregulation of VISTA expression by TGF-β.

3.2. *Smad3, TAK1 activity and ATF-2 differentially control expression of VISTA in different types of cells*

We were then looking to understand the biochemical mechanisms underlying differential VISTA expression responses to TGF-β. We exposed BEAS-2B cells to increasing concentrations of TGF-β and found that lower TGF-β concentrations (125 pg/ml) upregulated VISTA expression (which is in line with our previous observation [12]), then it comes back to the control level (at 250 pg/ml) followed by a gradual decrease (Fig. 4A and B). At the same time expression of galectin-9 gradually increases as well as do the levels of Tim-3-galectin-9 complex (Fig. 4A and B). Interestingly, kinase activity of TAK1 was increasing starting from the concentrations of TGF-β at which VISTA expression levels started decreasing (Fig. 4C). This was in line with upregulation of ATF-2 levels (Fig. 4C). We then checked 4 different cell types where we have seen upregulation or downregulation of VISTA expression upon exposure to TGF-β. All the cells were exposed to 2 ng/ml TGF-β for 16 h. We found that in the cells where TGF-β in the concentration 2 ng/ml induces increase in VISTA expression (LN-18

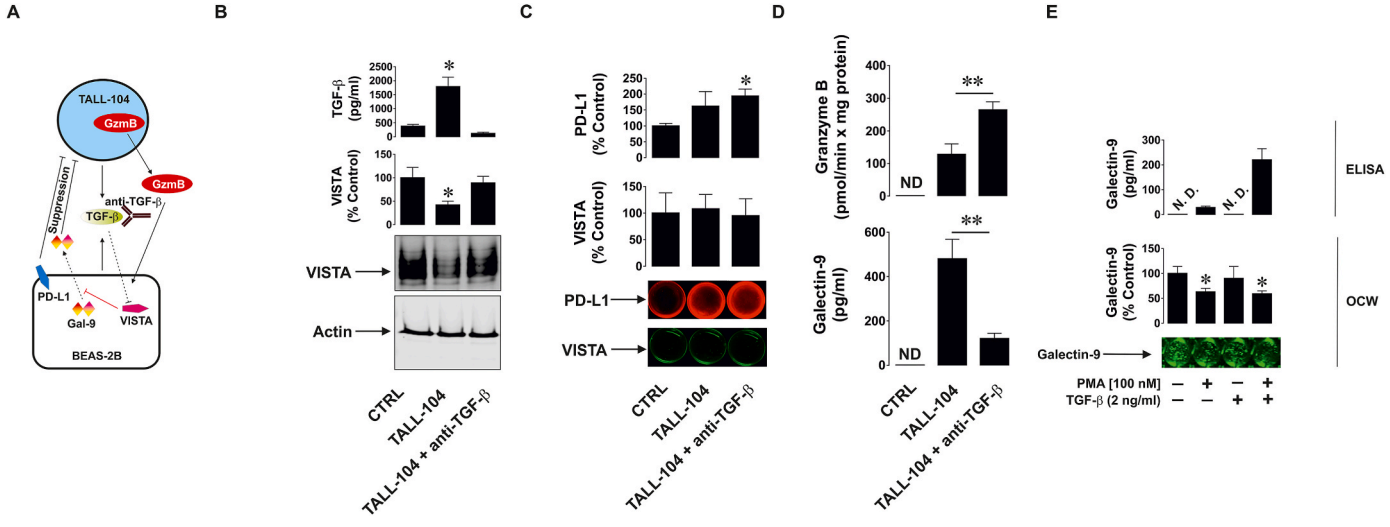


Fig. 2. TGF-β dependent suppression of VISTA expression stimulates galectin-9 secretion by BEAS-2B human bronchial epithelial cells. (A) BEAS-2B cells were co-cultured with TALL-104 cytotoxic T cells for 16 h in the ratio 1:1 with or without presence of TGF-β-neutralising antibody. **(B)** Following the co-culture described, BEAS-2B cells were washed, harvested, lysed and subjected to Western blot analysis of VISTA expression. TGF-β levels were measured in the medium by ELISA. **(C)** VISTA and PD-L1 levels were measured on the surface of BEAS-2B cells using on-cell Western analysis. **(D)** Granzyme B activity was analysed in BEAS-2B cells and, at the same time, levels of secreted galectin-9 were measured by ELISA in the culture medium. (E) BEAS-2B cells were treated with 100 nM PMA, 2 ng/ml TGF-β and combination of both for 16 h followed by detection of cell surface levels of galectin-9 in the cells and secreted galectin-9 levels in cell culture medium. Images are from 1 experiment representative of 5 which gave similar results. Quantitative data are mean values ± SEM of 5 independent experiments. *$p < 0.05$ and **$p < 0.01$ between indicated events or *vs* control.

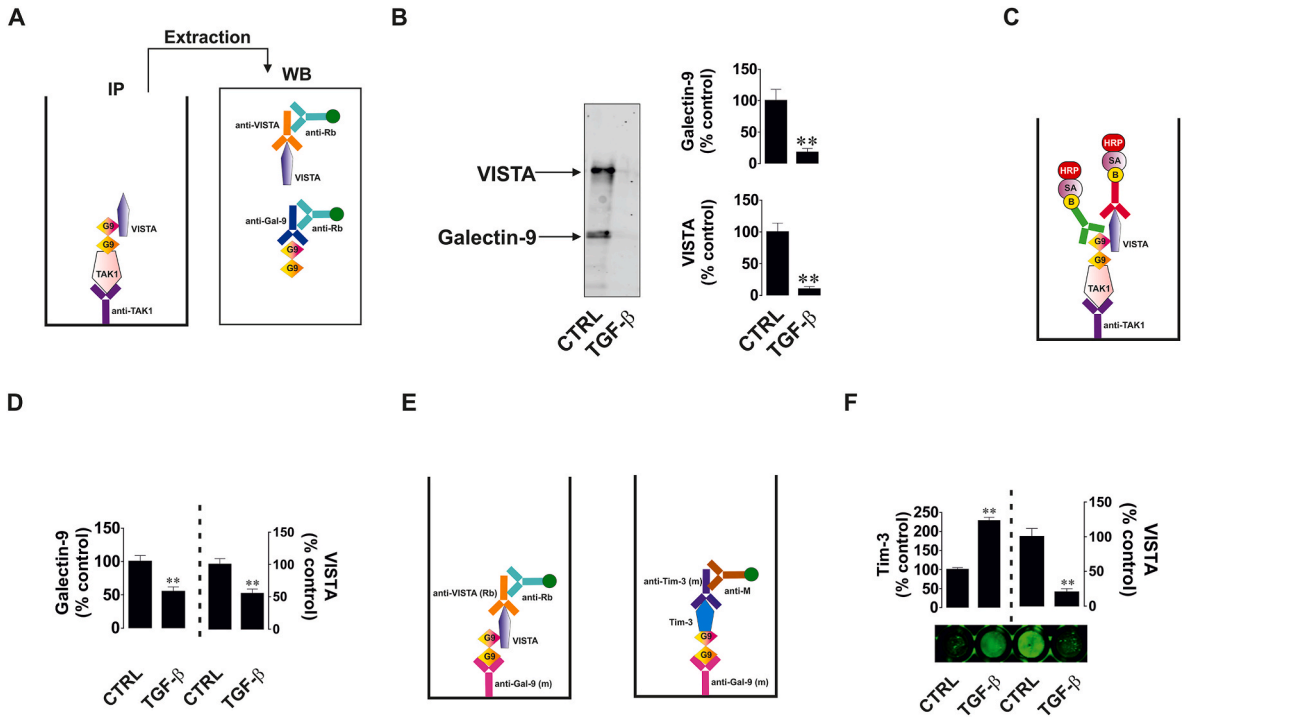


Fig. 3. VISTA facilitates intracellular interactions of galectin-9 with TAK1. (A) TAK1 was immunoprecipitated from resting and TGF-β-treated (16 h, 2 ng/ml) BEAS-2B cells (16 h, 2 ng/ml) using MaxiSorp plates and the precipitated proteins and subjected to further analysis: **(B)** extracted and analysed by Western blot or **(C)** and **(D)** analysed by ELISA to detect presence of galectin-9 and VISTA. **(E)** Galectin-9 was immunoprecipitated from resting and TGF-β-treated BEAS-2B cells (16 h, 2 ng/ml) using MaxiSorp plates and samples were subjected to detection of VISTA and Tim-3 by ELISA. Images are from 1 experiment representative of 5 which gave similar results. Quantitative data are mean values ± SEM of 5 independent experiments. **p < 0.01 vs control.

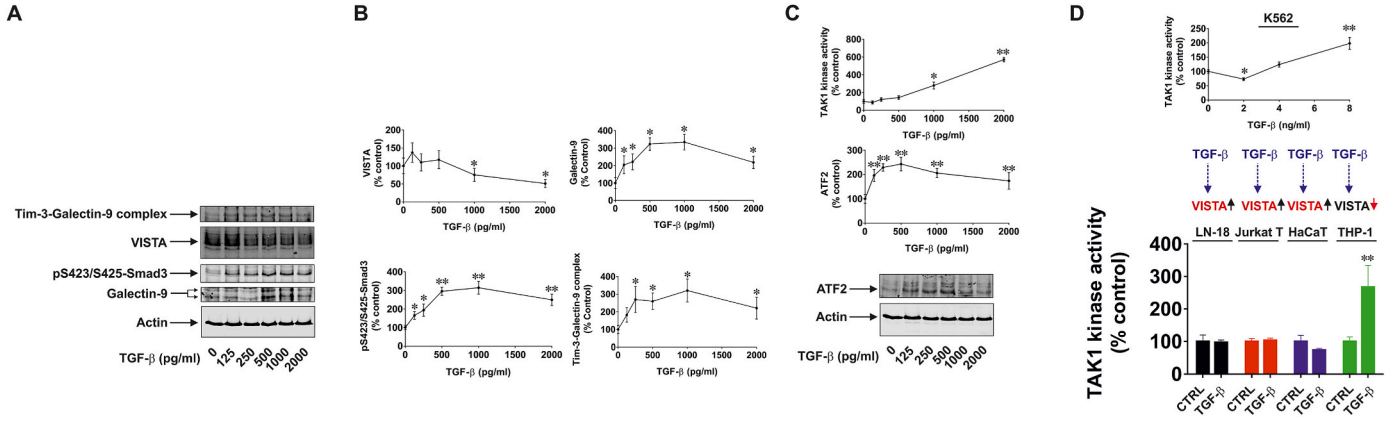


Fig. 4. TGF-β-induced downregulation of VISTA expression is in line with activation of TAK1. (A) BEAS-2B cells were exposed for 16 h to various concentrations of TGF-β followed by Western blot analysis of pS423/S425-Smad3, VISTA and galectin-9 expression levels. **(B)** Obtained results were quantitatively analysed. **(C)** ATF-2 expression levels were also measured by Western blot analysis; TAK1 kinase activity was analysed as outlined in Materials and Methods. **(D)** Lower panel: Resting and TGF-β-treated (16 h, 2 ng/ml) LN-18 (human high grade glioblastoma cells), Jurkat T (human T cell leukaemia cells) and HaCaT (human keratinocytes), which respond by upregulation of VISTA to TGF-β treatment and THP-1 human AML cells, where TGF-β downregulates VISTA expression were subjected to TAK1 kinase activity assay. Upper panel: K562 cells (which respond by upregulation of VISTA expression to treatment for 16 h with 2 ng/ml TGF-β and downregulation – to treatment for 16 h with 8 ng/ml TGF-β) were treated for 16 h with 2, 4 and 8 ng/ml TGF-β and TAK1 kinase activity was analysed. Images are from 1 experiment representative of 3 which gave similar results. Quantitative data are mean values ± SEM of 3–5 independent experiments. *p < 0.05 and **p < 0.01 vs control.

glioblastoma cells [14], Jurkat T cells [11] and HaCaT keratinocytes [11]), there was no increase in TAK1 kinase activity after exposure to TGF-β. While the cells which respond by downregulation of VISTA (THP-1) showed significant increase in TAK1 kinase activity when treated with TGF-β (Fig. 4C). In our recent work we have shown that in K562 chronic lymphoid leukaemia cells TGF-β induces expression of VISTA in the concentration 2 ng/ml [17]. However, further increase in TGF-β concentration reduces the effect. As such we sought to confirm that this is in line with changes in TAK1 activity and found that this is the case (Fig. 4C top panel). As such, we hypothesised that TAK1 induced activation of ATF-2 may lead to ATF-2-dependent repression of VISTA expression. By looking at VISTA gene (*VSIR*) promoter region we found an element with the sequence TAACGTCT, which is similar to the ATF-binding cite in granzyme B (TAACGTAA, while classic consensus sequence for CREB/ATF is 5′-TGACGTCA-3′) which was recently reported by other groups [24]. As such, we sought to understand which transcription factors and activating enzymes are responsible for TGF-β-induced downregulation of VISTA expression. We first knocked

down Smad3 in BEAS-2B cells and looked whether this would change TGF-β effect on VISTA expression. When we exposed Smad3 knock-down BEAS-2B cells to 2 ng/ml TGF-β for 16 h, downregulatory effect of VISTA was reduced compared to the wild-type cells and to BEAS-2B cells transfected with random siRNA (Fig. 5A). However, knocking down Smad3 did not restore control levels of VISTA which could be due to presence of ATF-2 in the cells, which TAK1 could have activated. However, when BEAS-2B cells were exposed to 2 ng/ml TGF-β for 16 h in the absence or presence of takinib (10 μM; highly specific TAK1 inhibitor), it was clear that takinib was able to completely restore VISTA expression levels back to those in resting cells. We therefore sought to confirm the role ATF-2 in TGF-β-induced repression of VISTA expression. We compared two genes – *LGALS9* (encodes galectin-9, which responds by upregulation of expression to treatment with TGF-β) and VISTA, where we see the opposite effect. *LGALS9* promoter region does not seem to contain response elements which can interact with ATF-2 (Fig. 5C). We exposed BEAS-2B cells to 2 ng/ml TGF-β for 16 h and performed ChIP followed by PCR using anti-Smad3 and anti-ATF-2 antibodies to immunoprecipitate chromatin. We found that exposure to TGF-β significantly upregulated enrichment of both *LGALS9* and *VSIR* with Smad3. However, there was now enrichment of *LGALS9* with ATF-2. But *VSIR* appeared to be enriched with ATF-2 upon exposure to TGF-β (Fig. 5D). At the same time, we confirmed that galectin-9 mRNA levels were significantly upregulated upon exposure to TGF-β while VISTA mRNA levels significantly went down (Fig. 5E). This confirms our hypothesis and highlights the role of TAK1-induced activation of ATF-2 in TGF-β-induced downregulation of VISTA expression.

3.3. *VISTA localisation and its intracellular and extracellular functions determine the way how its expression responds to TGF-β*

We sought to understand biological reasons for differential responses of VISTA expression to TGF-β shown by various types of cells. We used Calu6 pulmonary adenocarcinoma cells which have similar origin to BEAS-2B, but before they became a cell line, they were forming aggressive malignant tumour and thus were exposed to real TME. When these cells were exposed to TGF-β (2 ng/ml, 16 h), they responded by upregulation of both VISTA and galectin-9 expression (Fig. 6A). Notably, their background levels of VISTA were much lower compared to BEAS-2B cells (Fig. 6A). Calu6 also responded by upregulation of Tim-3 expression (Fig. 6B). But no changes in TAK1 activity or expression levels were detected (Fig. 6B). We looked at cell surface presence of VISTA in studied cell types using on-cell Western analysis. We investigated wild type BEAS-2B cells as well as BEAS-2B cells transformed to malignant cells *in vitro* using bracken fern alkaloid ptaquiloside. As a negative control we used MCF-7 human breast cancer cells which do not express VISTA at all. Calu6 cells were studied as well. In MCF-7 and wild type BEAS-2B cells we saw just a background signal (Fig. 6C). In transformed BEAS-2B cells a very slight upregulation of VISTA cell surface presence was observed (Fig. 6C). But in Calu6 VISTA was obviously present on the cell surface. This means that these small amounts of VISTA that were detected in Calu6 cells by Western blot, were translocated onto the cell surface (Fig. 6A). Obviously, Calu6 cells use VISTA mainly on the extracellular level as immune checkpoint protein rather than to facilitate galectin-9 interactions with TAK1.

Interestingly, when testing pulmonary carcinoma organoids obtained from patients against the organoids obtained from healthy lung tissue of the same patients, we found that VISTA levels were upregulated in cancer cells compared to healthy cells as well as was galectin-9 and Tim-3-galectin-9 complex (Supplementary Fig. 1), which suggest that observed effect takes place in primary human lung cancer (pulmonary carcinoma).

To investigate this further we used primary human embryonic cells obtained from patients at ca 13 (chorion) and ca 20 (amnion) weeks of pregnancy. Both cell types express TAK1 and the amounts detected are similar (Fig. 6D). We then used BEAS-2B, MCF-7 (no VISTA expression), Calu6 as well as primary human embryonic cells obtained as amnion and chorion stages and immunoprecipitated TAK1 as described above. We found that it was co-precipitated with galectin-9 in all the cases. However, in some cases VISTA was mainly accompanying galectin-9 while in MCF-7 cells it was solely Tim-3 (Fig. 6E and F). Importantly, Tim-3 can always be translocated onto the cell surface together with galectin-9 but partly can be localised inside the cell. While VISTA in some cell types does not get translocated onto the cell surface and as such could prevent galectin-9 secretion. Primary human embryonic cells obtained at chorion stage responded to TGF-β treatment (16 h, 2 ng/ml) by upregulation of both galectin-9 and VISTA levels (Fig. 6G). At the same time no upregulation of TAK1 activity was observed (Fig. 6G). On the other hand, cells obtained at amnion stage responded by upregulation of galectin-9 expression, while VISTA levels were downregulated (Fig. 6H). Exposure to TGF-β (16 h, 2 ng/ml) induced activation of TAK1 in these cells (Fig. 6H) showing changes in VISTA role during embryonic development.

We also tested primary healthy adult mouse organ homogenates for the presence of VISTA and found that this protein is present in all the organs. It can be present either in non-glycosylated, partially

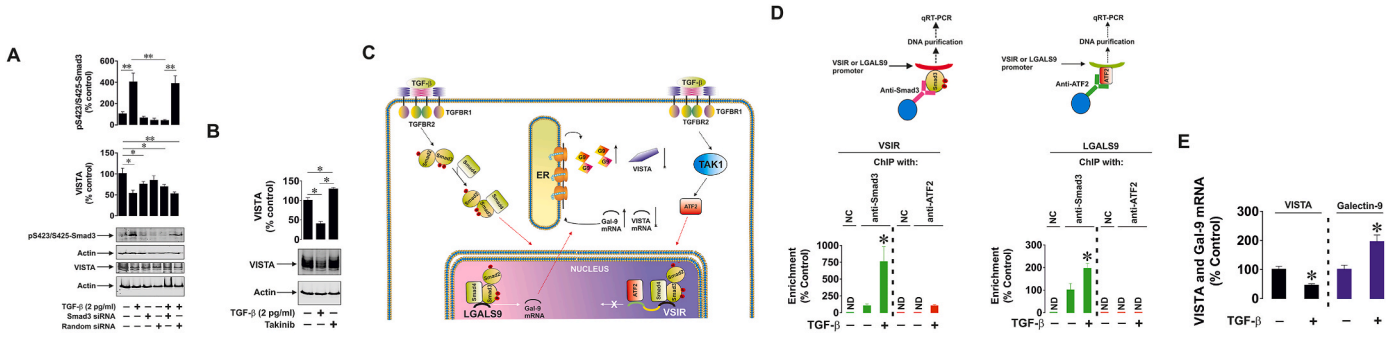


Fig. 5. ATF-2 can repress phospho-Smad3-induced expression of VISTA. (A) BEAS-2B cells were subjected to transfection with siRNA against Smad3 as well as random siRNA followed by exposure for 16 h to 2 ng/ml TGF-β. VISTA and pS423/S425-Smad3 expression levels were then analysed by Western blot. **(B)** BEAS-2B cells were exposed for 16 h to 2 ng/ml TGF-β with or without 1 h pre-treatment with 10 μM Takinib (TAK1 inhibitor). Expression levels of VISTA were analysed by Western blot. **(C)** Based on the results we hypothesised that phospho-Smad3-induced expression of VISTA can be repressed by ATF-2, while expression of other genes (e. g. *LGALS9*) which do not respond to ATF-2 keeps responding by upregulation. **(D)** We used resting BEAS-2B cells and those exposed to 2 ng/ml TGF-β for 16 h and subjected them to ChIP with anti-Smad3 and anti-ATF-2 antibodies, followed by qRT-PCR analysis of enrichment with fragments of *VSIR* (VISTA gene) promoter region fragments and *LGALS9* (galectin-9 gene) promoter regions. **(E)** Resting BEAS-2B cells and those exposed to 2 ng/ml TGF-β for 16 h were subjected to qRT-PCR analysis of VISTA and galectin-9 mRNA levels. Images are from 1 experiment representative of 3 which gave similar results. Quantitative data are mean values ± SEM of 3–5 independent experiments. *p < 0.05 and **p < 0.01 vs control.

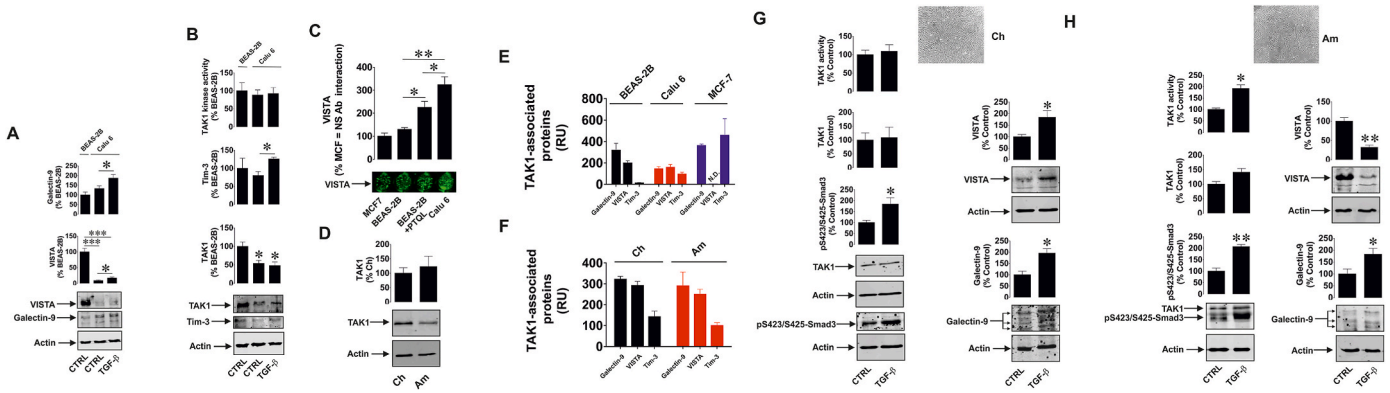


Fig. 6. VISTA expression is differentially controlled in human cancer and embryonic cells in response to exposure to TGF-β most likely depending on extra- and intracellular functions of VISTA in these cells. (A) Resting human BEAS-2B cells ("healthy control") as well as resting and TGF-β-treated (2 ng/ml for 16h) Calu6 human pulmonary carcinoma cells were subjected to Western blot analysis of VISTA and galectin-9 expression levels. **(B)** Levels of Tim-3 and TAK1 as well as TAK1 kinase activity were also investigated. **(C)** MCF-7 human breast cancer cells (lack VISTA expression), normal BEAS-2B, BEAS-2B cells transformed with ptaquiloside (PTQL) as well as Calu6 cells were subjected to analysis of VISTA cell surface levels using on-cell Western analysis. **(D)** TAK1 expression was analysed in primary human embryonic cells (chorion stage – Ch and amnion stage – Am) by Western blot. **(E)** TAK1 was immunoprecipitated from BEAS-2B, Calu6 and MCF-7 cells as well as **(F)** primary human embryonic cells. Association of galectin-9, VISTA and Tim-3 with immunoprecipitated TAK1 was analysed by ELISA. **(G)** Primary human embryonic cells (chorion stage - ca 13 weeks of pregnancy) were exposed to 2 ng/ml of TGF-β for 16 h. Phospho-Smad3 and TAK1 expressions as well as TAK1 kinase activity were analysed. Also expressions of galectin-9 and VISTA were assessed. **(H)** Primary human embryonic cells (amnion stage - ca 20–22 weeks of pregnancy) were exposed to 2 ng/ml of TGF-β for 16 h. Phospho-Smad3 and TAK1 expressions as well as TAK1 kinase activity were analysed. Also expressions of galectin-9 and VISTA were assessed. Images are from 1 experiment representative of 4 which gave similar results. Quantitative data are mean values ± SEM of 4 independent experiments. *$p < 0.05$; **$p < 0.01$ and ***$p < 0.001$ vs control or between indicated events.

glycosylated and/or fully glycosylated form (Supplementary Fig. 2). This confirms that VISTA has functions in all the tissues unlike it was thought to have one mainly in leukocytes.

However, the effects observed in Calu6 cells do not mean that all cancer cells which express VISTA will use it as immune checkpoint and not just for facilitating galectin-9 interactions with TAK1 or other possible intracellular functions which may be discovered in the future. As example, HuH7 hepatocellular carcinoma cells which express relatively high levels of VISTA respond to 16 h of exposure to 2 ng/ml TGF-β by downregulation of VISTA expression and upregulation of galectin-9, which forms complex with Tim-3 (Supplementary Fig. 3A and B and C). In HuH7 cells, TAK1 activation was also observed (Supplementary figure 3 B), which is in line with the observations reported above. Importantly, resting HuH7 cells do not secrete galectin-9, while upon co-culturing them with Jurkat T cells in the ratio 1:1 for 16 h we found that the levels of soluble TGF-β remain unchanged while the levels of TGF-β based on the HuH7 surface (those bound to TGF-β receptors) were significantly increased (Supplementary Fig. 3D). Upon removal of the T cells and replacement of the culture medium HuH7 cells kept heavily secreting galectin-9 via the mechanisms described before (Supplementary Fig. 3E).

We then sought to verify our findings in primary human cancers which express VISTA. In human colorectal cancer liver metastatic tumours (CRCLM, samples obtained from 2 patients) we saw downregulation of VISTA compared to healthy liver tissues (Supplementary Figs. 4A and B). At the same time, the levels of phospho-Smad3 (measured by Western blot) and TGF-β (measured by ELISA) were significantly upregulated in the tumour (Supplementary Figs. 4A and C). Obviously T cells were infiltrating the tumour given the levels of CD3 observed in malignant tissue compared to the healthy one (Supplementary Fig. 4 A and C). Tim-3 levels were significantly upregulated in tumour as well (Supplementary Fig. 4A and B). Importantly, TAK1 activity was significantly increased in tumours compared to healthy tissues (Supplementary Fig. 4B). At the same time, studied patients showed much higher levels of galectin-9 in blood plasma compared to healthy donors (Supplementary Fig. 5) which supports the concept regarding the role of VISTA in facilitation of intracellular interactions of galectin-9 with TAK1.

On the other hand, primary human breast carcinomas showed higher expression levels of VISTA compared to healthy breast tissues of the same patients (Supplementary Fig. 6A and B). The same effect was applicable to galectin-9 (Supplementary Fig. 6A and B). At the same time, TGF-β (measured by ELISA) and phospho-Smad3 (measured by Western blot) levels were significantly upregulated in tumours as well (Supplementary Fig. 6 A, C and D). Levels of CD3 were also significantly increased in the tumour (Supplementary Fig. 6 A and C) suggesting that T cells were infiltrated into the tumours. Interestingly, that blood plasma galectin-9 levels of breast carcinoma patients were not very different from healthy donors, which is in line with our previous observation. Based on these results one could assume that breast carcinomas expressing VISTA studied in this work use VISTA as immune checkpoint protein in the TME.

Importantly, we found that in some cell types, which can translocate VISTA onto the surface, TGF-β can not only trigger upregulation of VISTA expression, but also increase its secretion. As we know from our previous work, VISTA secretion is associated with proteolytic shedding of the extracellular domain off the cell surface. We found that pancreatic ductal adenocarcinoma (PDAC) cells PANC-1, respond by activation of Smad3 but not TAK1 to 16 h treatment with 2 ng/ml TGF-β (Supplementary Fig. 7A). This corresponds to increase in galectin-9 expression and no changes in the levels of cell-associated Tim-3 or VISTA (Supplementary Fig. 7B). VISTA is obviously present on the cell surface of PANC-1 cells, however its amount on the cell surface is non-significantly reduced upon exposure to TGF-β (Supplementary Fig. 7C). At the same time, exposure to TGF-β triggers VISTA secretion, which is significantly upregulated following 16 h of exposure to 2 ng/ml TGF-β (Supplementary Fig. 7C). This means the increase in total VISTA expression upon exposure to TGF-β. No other cell types, which we studied (as described above) were found to upregulate VISTA secretion in response to TGF-β. Also, resting and TGF-β-treated PANC-1 cells secreted barely detectable amounts of galectin-9 (interestingly, it was significantly upregulated by exposure to TGF-β, but still very minor release was detected), see Supplementary Fig. 7C. In PANC-1 cells TGF-β also significantly upregulates PD-L1 expression and its translocation onto the cell surface (Supplementary Fig. 7C). Interestingly, these cells also produce and secrete relatively high levels of L-kynurenine, which do not anyhow respond to TGF-β treatment, confirming the evidence shown in protein atlas database, that PANC-1 cells express tryptophan

dioxygenase (TDO) and not indoleamine-2,3-dioxygenase 1 (IDO1), and making sure stable contribution of L-kynurenine to supporting immunosuppressive TME (Supplementary Fig. 7D). Importantly, when co-cultured with Jurkat T cells as described before [14] and above (Supplementary Fig. 3), PANC-1 cells secrete high levels of galectin-9 (Supplementary Fig. 7E). These results confirm that PDAC PANC-1 cells use VISTA as immune checkpoint protein as a part of their immune evasion machinery. In is important to stress that our results show that these PDAC cells operate several "layers" of development of immunosuppressive tumour microenvironment unlike other cells/tumours we studied. They secrete galectin-9 and VISTA thus disabling T cells (this mechanism we have reported before [6,14]). At the same time, constantly high levels of secreted L-kynurenine are used to permanently support immunosuppressive TME. In the case when direct attack by T cells still takes place, high cell surface levels of PD-L1 observed on these cells will protect them (schematically this is reflected in Supplementary Fig. 7F). These results shed the light on why pancreatic cancers often do not respond to immunotherapies and are so successful in progressing the disease and respectively, are notoriously hard to treat. This is also a classic example of VISTA playing active role in complex immune evasion machinery rather than being intracellular facilitator of galectin-9-TAK1 interactions, as we have shown above for other cell types including some of the cancers.

3.4. ATF-2 is also capable of suppressing VISTA expression induced by HIF-1 transcription complex

Recent evidence has clearly demonstrated that HIF-1 transcription complex is capable of upregulating VISTA expression in human cells [13]. We asked whether ATF-2 can still suppress HIF-1-induced VISTA expression or if this effect is only applicable to Smad-3-induced process. To investigate this, we used BEAS-2B cells, HaCaT keratinocytes and THP-1 acute myeloid leukaemia cells, which express high levels of VISTA and exposed them for 4 h to 50 μM $CoCl_2$ in the presence of TGF-β neutralising antibody. This is done to rule out any possibility of autocrine action of TGF-β, expression of which can be induced by HIF-1. On one hand, $CoCl_2$ induces HIF-1 activation by blocking HIF-1α prolyl hydroxylation. On the other hand, $ColCl_2$ inhibits superoxide dismutase activity (SOD) [25,26] thus leading to upregulation of reactive oxygen species (ROS)-dependent activation of apoptosis signal regulating kinase 1 (ASK1), which is known to activate ATF-2 [21] (schematically, these processes are shown in Fig. 7A). The intensity of this effect may vary depending on the type of cells. We found that in BEAS-2B cells exposed to $CoCl_2$, TBRS levels (showing the effects of ROS) and respectively ASK1 activity levels were significantly increased (Fig. 7B). These effects were not observed in other cell types investigated (Fig. 7B). Importantly, in BEAS-2B cells $CoCl_2$ induced clear activation of HIF-1 and downregulation of VISTA, which was not as strong as the one induced by TGF-β (Supplementary Figs. 8A and B). However, in THP-1 cells, TGF-β induced downregulation of VISTA, but $CoCl_2$-induced activation of HIF-1 was in line with increased VISTA expression (Supplementary Figs. 8C and D). In HaCaT cells, both TGF-β and $CoCl_2$/HIF-1 induced clear upregulation of VISTA expression (Supplementary Figs. 8E and F). Neither BEAS-2B nor THP-1 cells were able to secrete detectable amounts of secreted VISTA. HaCaT secreted VISTA, but this process was not significantly affected neither by $CoCl_2$ nor by TGF-β (unlike in pancreatic cancer cells, Supplementary Fig. 8A, C and E). Obviously, $CoCl_2$-dependent downregulation of VISTA was observed only in the cells, where $ColCl_2$ upregulated ASK1 activity (BEAS-2B). We have then performed ChIP followed by qRT-PCR using both anti-HIF-1 and anti-ATF-2 antibodies. In all 3 cell types $CoCl_2$ upregulated enrichment, which means HIF-1 was interacting with promoter region of VISTA in all 3 cell types. With anti-ATF-2, we observed $CoCl_2$-upregulated enrichment only in BEAS-2B cells, suggesting that ATF-2 was responsible for downregulation of VISTA expression (all these results are shown in Fig. 7C). Finally, we wanted to rule out the downregulatory effect of HIF-1 itself and further confirm the role of ASK1. We exposed BEAS-2B cells to $CoCl_2$ in the presence of TGF-β neutralising antibody with or without pre-transfection of the cells with dominant-negative form of ASK1 (ΔN-ASK1). Alternatively, we exposed the cells for 4 h to hypoxia (1 % oxygen). This was followed by measurement of VISTA expression by Western blot analysis. We found that dominant-negative ASK1 attenuated downregulation of VISTA expression induced by $CoCl_2$, confirming our findings. And importantly, hypoxia itself induced upregulation of VISTA in BEAS-2B cells further confirming obtained results (Fig. 7D). All the treatments highly upregulated HIF-1 DNA-binding activity (Fig. 7E).

As such, VISTA expression is thoroughly regulated by a set of transcriptional control systems due to multiple intra- and extracellular functions of this protein.

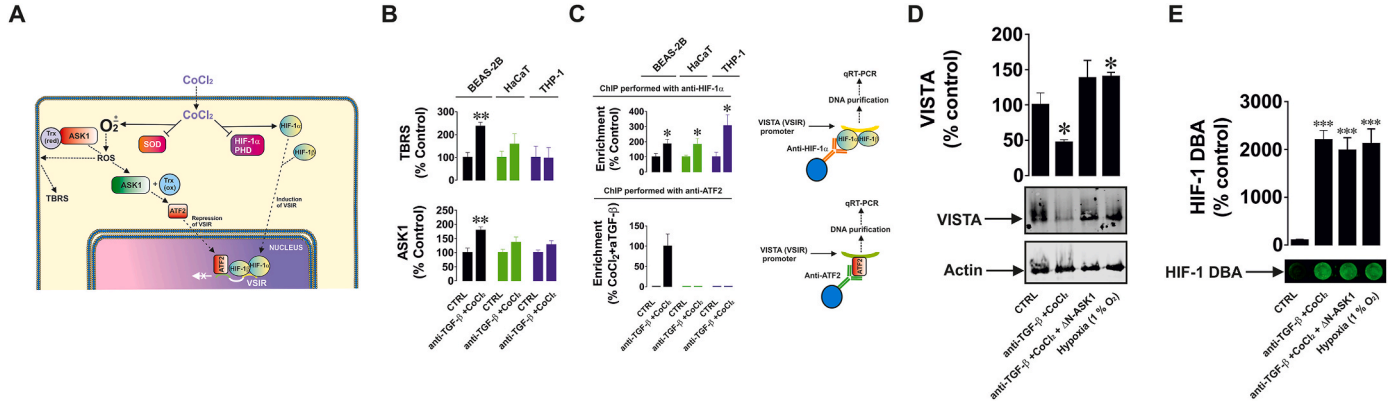


Fig. 7. ATF-2 is capable of suppressing HIF-1-induced VISTA expression. (A) In order to test if ATF-2 activated by ASK1 pathway (induced via redox-dependent mechanism) is capable of suppressing VISTA expression we investigated the effect of cobalt chloride-induced HIF-1 activation (which can be associated with heavy production of reactive oxygen species (ROS) and thus ASK1/ATF-2 activation) on VISTA expression. **(B)** BEAS-2B, HaCaT and THP-1 cells were exposed for 16 h to 50 μM cobalt chloride and TGF-β-neutralising antibody. Kinase activity of ASK1 and TBRS levels were analysed in cell lysates. **(C)** ChIP followed by qRT-PCR was performed using anti-HIF-1α and anti-ATF-2 antibodies in resting and $CoCl_2$/TGF-β-neutralising antibody treated BEAS-2B, HaCaT and THP-1 cells. Enrichment with fragments of *VSIR* (VISTA gene) promoter regions was analysed using qRT-PCR. **(D)** Resting or transfected with ΔN-ASK1 BEAS-2B cells were exposed for 4 h to 50 μM cobalt chloride and TGF-β-neutralising antibody. As additional control we also used BEAS-2B cells exposed to hypoxia (1 % oxygen) for 4 h. VISTA expression was analysed in all the cells by Western blot. **(E)** In the cells described in section D we also measured HIF-1 DNA-binding activity by ELISA-based method. Images are from 1 experiment representative of 4 which gave similar results. Quantitative data are mean values ± SEM of 4 independent experiments. *$p < 0.05$; **$p < 0.01$ and ***$p < 0.001$ vs control.

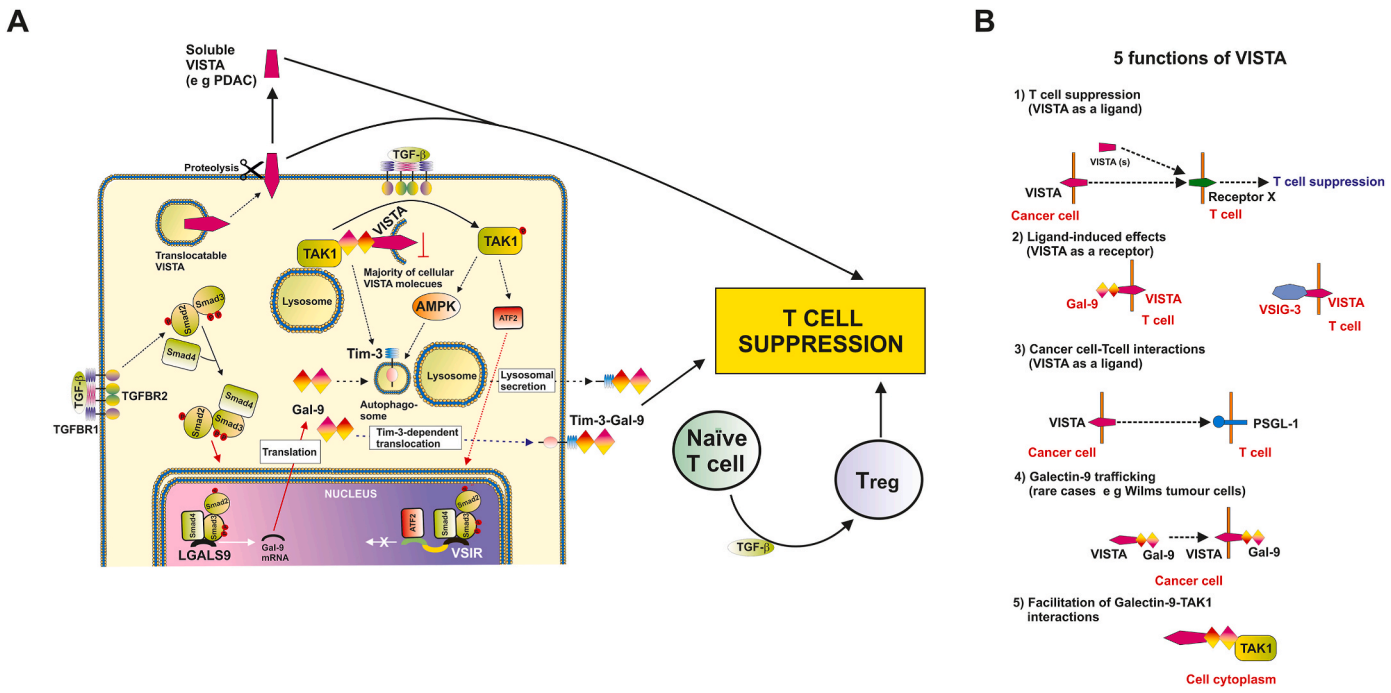


Fig. 8. Extracellular and intracellular functions of VISTA. (A) Scheme illustrating intracellular and extracellular activities of VISTA. **(B)** Illustration of 5 different possible functions of VISTA.

4. Discussion

In this work we sought to study cell type-specific approaches to regulation of VISTA expression, which are dictated by extra- and intracellular functions of this multifunctional protein. We reported before and confirmed here, that VISTA expression can be upregulated or downregulated by TGF-β depending on the cell type [11,14]. The biological reason for this phenomenon and molecular mechanisms underlying it remain unclear. Here we found that in the cells, which use VISTA mainly as intracellular protein (BEAS-2B, THP-1 AML monocytes), TGF-β downregulates VISTA expression. Furthermore, we found that VISTA in these cells engages in intracellular interactions with galectin-9 facilitating interaction of galectin-9 with TAK1. As we know, galectin-9 lacks secretion sequence (signal domain) [14,17,19], and as such, needs to engage with carrier proteins in order to control its distribution. Recent evidence demonstrated that galectin-9 interactions with TAK1 are crucially important for lysosome protection and also for AMP kinase (AMPK)-dependent activation of autophagy [26–29]. Galectin-9-TAK1 interactions may contribute to regulation of TAK1 kinase activity, which is engaged in protection of lysosomes and control of autophagy through AMPK [26–29].

Action of TGF-β most likely leads to direct TGF-β-dependent activation of TAK1. Downregulation of VISTA results in newly formed galectin-9 to interact with Tim-3 for the purpose of translocation onto the surface or engagement in lysosomal secretion, as we have recently reported [14]. This has clear biological sense since increase in TGF-β for cancer cells forming TME means immune attack, which requires action of immune evasion machinery. As a part of this process, galectin-9 needs to be secreted, and when highly expressed VISTA is not secreted or translocated onto the cell surface in the cells, it means that galectin-9 secretion will be affected, which obviously cancer cells would need to avoid.

As we have seen, this process is common for non-malignant cells, some of the cancer cells with high expression levels and low surface presence of VISTA (hepatocellular carcinoma) and embryonic cells at later stages (amnion stage) of pregnancy.

However, many cancer cells (e g lung cancer, breast cancer, pancreatic cancer) are capable of translocating VISTA onto the surface and thus will not prevent galectin-9 secretion. These cells also express lower absolute amounts of VISTA. Such cells will respond to exposure to TGF-β by upregulation of VISTA expression, since they may actively use VISTA as immune checkpoint protein engaged in immune evasion. This effect is also applicable to non-malignant cells. Interestingly, we observed this for rapidly proliferating cells, like HaCaT keratinocytes and primary human embryonic cells at earlier stages (chorion stage) of pregnancy, when mother's immune system tries to reject the embryo and thus, it has to suppress anti-embryonic activities of mother's T and NK cells [17]. These cells respond to TGF-β by upregulation of VISTA expression and translocate VISTA onto the cell surface, most likely using it as immune checkpoint protein.

Our results have shown that TAK1 activation by TGF-β leads to activation of ATF2, which then interacts with promoter region of *VSIR* (VISTA encoding gene) and most likely represses it. Our suggestion is that ATF-2 binds to the response element in *VSIR* which is very similar to ATF-binding site in promoter region of granzyme B gene [30]. TGF-β/TAK1-induced ATF-1 interacts with promoter region of granzyme B and suppresses expression of this gene [30]. We have now observed the same effect with TGF-β/TAK1-induced ATF-2, when it represses phospho-Smad3-induced activation of VISTA expression. In the cells, which respond by downregulation of VISTA expression to exposure to 2 ng/ml TGF-β (BEAS-2B) lower concentrations of TGF-β can still induce VISTA expression as we have seen here and also reported before. Taken together, our results suggest that each type of malignant and non-malignant cells have their threshold of TGF-β concentration required to activate TAK1. It is very high for cancer and embryonic cells using VISTA as immune checkpoint protein and translocating it onto the cell surface or even releasing it (PDAC), where VISTA contributes to development of immunosuppressive TME or defends the cells against immune attack. Interestingly, for keratinocytes (results observed in HaCaT cells) such immunosuppressive activity of VISTA may explain the ability of keratinocytes to defend against cytotoxic T cells and respond by abnormal proliferation to T cell attack observed in the case of psoriasis or similar types of autoimmune disease. Importantly, ATF-2 is also capable of suppressing HIF-1-induced expression of VISTA, which means

that VISTA gene, regardless of presence of activating transcription factors is repressed by ATF-2. Furthermore, our results have demonstrated that both Smad3 and HIF-1 are bound to VISTA promoter region when ATF-2 interacts with it.

Our work also led to a very important observation that most of healthy human and mammalian (mouse) tissues express VISTA. We saw clear VISTA expression in healthy human lung, breast and liver tissue as well as in majority all mouse organs/tissues we were able to investigate. Also, primary human embryonic cells expressed high levels of VISTA, however, at earlier stage of pregnancy (chorion stage – ca 13 weeks of pregnancy), it is mainly used as immune checkpoint protein as we have seen here and also in our previous work. But, at later stages (amnion stage – ca 23 weeks of pregnancy), where suppression of immune attack by mothers immune system becomes less critical, VISTA expression is suppressed by TGF-β (Fig. 6).

Overall, taking together results of this work and previous reports one could clearly see that VISTA has both extra- and intracellular functions.

Observed intracellular functions include facilitation of galectin-9 interactions with TAK1 and, in rare cases, trafficking of galectin-9 for conducting immunosuppressive functions (Wilms tumour cells) [14]. Extracellular functions of VISTA include the effects of VISTA translocated onto the cells surface or then secreted (shed off the surface) [6,15]. This is mainly associated with suppression of cytotoxic T cell functions. Schematically these functions of VISTA are demonstrated in Fig. 8A and specific VISTA functions are illustrated in Fig. 8B. Previous work highlighted that VISTA can also act as a T cells receptor through which T cell function can be downregulated [6,14]. Importantly, similar effects of other proteins on facilitation of intracellular galectin-9 functions were also observed [31]. For example, recent evidence demonstrated the role of vesicle-associated membrane protein 3 (Vamp-3) in facilitation of galectin-9 activity of regulation of cytokine secretion in dendritic cells [31]. Our work therefore highlighted the intracellular and extracellular functions of VISTA. Localisation of VISTA determines the type of activity in which it engages (extracellular or intracellular). Different types of cancer cells exhibit differential VISTA functions. As such, the expression of VISTA is differentially regulated by immunosuppressive TME factors such as TGF-β and hypoxic signalling. In cases when VISTA plays mainly the role as immune checkpoint protein, the upregulation will be observed in both cell lines and primary tumours (e.g. lung or breast cancer). However, if VISTA mainly plays intracellular role discovered in this work (e. g. hepatocellular carcinoma, colorectal cancer liver metastasis), VISTA expression will be downregulated by TGF-β. Taken together, our work highlights a major role of VISTA in support of normal cell homeostasis as well as cancer progression/immune evasion.

CRediT authorship contribution statement

Maryam Abooali: Validation, Methodology, Investigation, Conceptualization. **Stephanie Schlichtner:** Validation, Methodology, Investigation. **Xi Lei:** Investigation. **Nijas Aliu:** Methodology, Investigation. **Sabrina Ruggiero:** Methodology, Investigation. **Sonia Loges:** Supervision. **Martin Ziegler:** Resources, Methodology. **Franziska Hertel:** Resources, Methodology. **Anna-Lena Volckmar:** Resources. **Albrecht Stenzinger:** Resources. **Petros Christopoulos:** Resources. **Michael Thomas:** Resources. **Elena Klenova:** Resources, Methodology. **N. Helge Meyer:** Resources, Methodology. **Stergios Boussios:** Conceptualization. **Nigel Heaton:** Resources. **Yoh Zen:** Resources. **Ane Zamalloa:** Resources. **Shilpa Chokshi:** Resources, Methodology. **Luca Urbani:** Resources, Methodology. **Sophie Richard:** Resources, Methodology. **Kavitha Kirubendran:** Resources, Methodology. **Rohanah Hussain:** Conceptualization. **Giuliano Siligardi:** Conceptualization. **Dietmar Cholewa:** Resources, Conceptualization. **Steffen M. Berger:** Supervision, Resources, Funding acquisition. **Inna M. Yasinska:** Writing – review & editing, Methodology, Investigation, Conceptualization. **Elizaveta Fasler-Kan:** Writing – review & editing, Supervision, Resources, Methodology, Investigation, Funding acquisition, Data curation, Conceptualization. **Vadim V. Sumbayev:** Writing – original draft, Supervision, Resources, Project administration, Methodology, Investigation, Funding acquisition, Data curation, Conceptualization.

Declaration of competing interest

The authors declare that they have no known competing financial interests or personal relationships that could have appeared to influence the work reported in this paper.

Acknowledgements

We thank Diamond Light Source for access to the B23 beamline and funding projects SM24509, SM20755, and SM21202). This work was also supported by a Swiss Batzebär grant (to EF-K and SB) and Chinese Council PhD Scholarship (XL).

Appendix A. Supplementary data

Supplementary data to this article can be found online at https://doi.org/10.1016/j.canlet.2025.217581.

References

[1] O. Kyrysyuk, K.W. Wucherpfennig, Designing cancer immunotherapies that engage T cells and NK cells, Annu. Rev. Immunol. 41 (2023) 17–38, https://doi.org/10.1146/annurev-immunol-101921-044122.
[2] V.V. Sumbayev, B.F. Gibbs, E. Fasler-Kan, Editorial: pathological reactions of cytotoxic lymphoid cells as universal therapeutic targets in cancer and autoimmune disease, Front. Med. 10 (2023) 1186318, https://doi.org/10.3389/fmed.2023.1186318.
[3] S. Schlichtner, et al., L-Kynurenine participates in cancer immune evasion by downregulating hypoxic signaling in T lymphocytes, OncoImmunology 12 (2023) 2244330, https://doi.org/10.1080/2162402X.2023.2244330.
[4] J.L. Lines, et al., VISTA is an immune checkpoint molecule for human T cells, Cancer Res. 74 (2014) 1924–1932, https://doi.org/10.1158/0008-5472.CAN-13-1504.
[5] J.L. Lines, L.F. Sempere, T. Broughton, L. Wang, R. Noelle, VISTA is a novel broad-spectrum negative checkpoint regulator for cancer immunotherapy, Cancer Immunol. Res. 2 (2014) 510–517, https://doi.org/10.1158/2326-6066.CIR-14-0072.
[6] I.M. Yasinska, et al., Ligand-receptor interactions of galectin-9 and VISTA suppress human T lymphocyte cytotoxic activity, Front. Immunol. 11 (2020) 580557, https://doi.org/10.3389/fimmu.2020.580557.
[7] N. Shekari, et al., VISTA and its ligands: the next generation of promising therapeutic targets in immunotherapy, Cancer Cell Int. 23 (2023) 265, https://doi.org/10.1186/s12935-023-03116-0.
[8] J. Wang, et al., VSIG-3 as a ligand of VISTA inhibits human T-cell function, Immunology 156 (2019) 74–85, https://doi.org/10.1111/imm.13001.
[9] Y. Deng, et al., Eliminating a barrier: aiming at VISTA, reversing MDSC-mediated T cell suppression in the tumor microenvironment, Heliyon 10 (2024) e37060, https://doi.org/10.1016/j.heliyon.2024.e37060.
[10] R.J. Johnston, et al., VISTA is an acidic pH-selective ligand for PSGL-1, Nature 574 (2019) 565–570, https://doi.org/10.1038/s41586-019-1674-5.
[11] S. Schlichtner, et al., Expression of the immune checkpoint protein VISTA is differentially regulated by the TGF-beta1 - Smad3 signaling pathway in rapidly proliferating human cells and T lymphocytes, Front. Med. 9 (2022) 790995, https://doi.org/10.3389/fmed.2022.790995.
[12] M. Abooali, et al., Activation of immune evasion machinery is a part of the process of malignant transformation of human cells, Transl Oncol 39 (2024) 101805, https://doi.org/10.1016/j.tranon.2023.101805.
[13] J. Deng, et al., Hypoxia-induced VISTA promotes the suppressive function of myeloid-derived suppressor cells in the tumor microenvironment, Cancer Immunol. Res. 7 (2019) 1079–1090, https://doi.org/10.1158/2326-6066.CIR-18-0507.
[14] S. Schlichtner, et al., T lymphocytes induce human cancer cells derived from solid malignant tumors to secrete galectin-9 which facilitates immunosuppression in cooperation with other immune checkpoint proteins, J Immunother Cancer 11 (2023), https://doi.org/10.1136/jitc-2022-005714.
[15] G.A. Noubissi Nzeteu, et al., Macrophage differentiation and polarization regulate the release of the immune checkpoint protein V-domain Ig suppressor of T cell activation, Front. Immunol. 13 (2022) 837097, https://doi.org/10.3389/fimmu.2022.837097.
[16] A. Prokhorov, et al., The immune receptor Tim-3 mediates activation of PI3 kinase/mTOR and HIF-1 pathways in human myeloid leukaemia cells, Int. J. Biochem. Cell Biol. 59 (2015) 11–20, https://doi.org/10.1016/j.biocel.2014.11.017.

[17] A.T.H. Selno, et al., Transforming growth factor beta type 1 (TGF-beta) and hypoxia-inducible factor 1 (HIF-1) transcription complex as master regulators of the immunosuppressive protein galectin-9 expression in human cancer and embryonic cells, Aging (Albany NY) 12 (2020) 23478–23496, https://doi.org/10.18632/aging.202343.
[18] S. Schlichtner, et al., Functional role of galectin-9 in directing human innate immune reactions to Gram-negative bacteria and T cell apoptosis, Int. Immunopharmacol. 100 (2021) 108155, https://doi.org/10.1016/j.intimp.2021.108155.
[19] I. Goncalves Silva, et al., The tim-3-galectin-9 secretory pathway is involved in the immune escape of human acute myeloid leukemia cells, EBioMedicine 22 (2017) 44–57, https://doi.org/10.1016/j.ebiom.2017.07.018.
[20] J. Ye, Y. Han, C. Wang, W. Yu, Cytoprotective effect of polypeptide from Chlamys farreri on neuroblastoma (SH-SY5Y) cells following HO exposure involves scavenging ROS and inhibition JNK phosphorylation, J. Neurochem. 111 (2009) 441–451, https://doi.org/10.1111/j.1471-4159.2009.06328.x.
[21] M. Saitoh, et al., Mammalian thioredoxin is a direct inhibitor of apoptosis signal-regulating kinase (ASK) 1, EMBO J. 17 (1998) 2596–2606, https://doi.org/10.1093/emboj/17.9.2596.
[22] V.V. Sumbayev, LPS-induced Toll-like receptor 4 signalling triggers cross-talk of apoptosis signal-regulating kinase 1 (ASK1) and HIF-1alpha protein, FEBS Lett. 582 (2008) 319–326, https://doi.org/10.1016/j.febslet.2007.12.024.
[23] L. Zhai, et al., Quantification of Ido1 enzyme activity in normal and malignant tissues, Methods Enzymol. 629 (2019) 235–256, https://doi.org/10.1016/bs.mie.2019.07.006.
[24] D.A. Thomas, J. Massague, TGF-beta directly targets cytotoxic T cell functions during tumor evasion of immune surveillance, Cancer Cell 8 (2005) 369–380, https://doi.org/10.1016/j.ccr.2005.10.012.
[25] V.K. Tripathi, S.A. Subramaniyan, I. Hwang, Molecular and cellular response of Co-cultured cells toward cobalt chloride (CoCl(2))-induced hypoxia, ACS Omega 4 (2019) 20882–20893, https://doi.org/10.1021/acsomega.9b01474.
[26] T. Kamiya, et al., Cobalt chloride decreases EC-SOD expression through intracellular ROS generation and p38-MAPK pathways in COS7 cells, Free Radic. Res. 42 (2008) 949–956, https://doi.org/10.1080/10715760802566566.
[27] J. Jia, et al., Galectins control mTOR in response to endomembrane damage, Mol. Cell 70 (2018) 120–135, https://doi.org/10.1016/j.molcel.2018.03.009, e128.
[28] J. Jia, et al., Galectins control MTOR and AMPK in response to lysosomal damage to induce autophagy, Autophagy 15 (2019) 169–171, https://doi.org/10.1080/15548627.2018.1505155.
[29] J. Jia, et al., AMPK, a regulator of metabolism and autophagy, is activated by lysosomal damage via a novel galectin-directed ubiquitin signal transduction system, Mol. Cell 77 (2020) 951–969, https://doi.org/10.1016/j.molcel.2019.12.028, e959.
[30] X. Wu, et al., Sensing of mycobacterial arabinogalactan by galectin-9 exacerbates mycobacterial infection, EMBO Rep. 22 (2021) e51678, https://doi.org/10.15252/embr.202051678.
[31] R. Santalla Mendez, et al., Galectin-9 interacts with Vamp-3 to regulate cytokine secretion in dendritic cells, Cell. Mol. Life Sci. 80 (2023) 306, https://doi.org/10.1007/s00018-023-04954-x.